PERGAMON

International Journal of Heat and Mass Transfer 45 (2002) 5091–5105

International Journal of HEAT and MASS TRANSFER

www.elsevier.com/locate/ijhmt

Experimental study of mixed convection and pressure drop in helically dimpled tubes for laminar and transition flow

Pedro G. Vicente *, Alberto García, Antonio Viedma

Department of Thermal and Fluids Engineering, Universidad Politécnica de Cartagena, Campus de la Muralla del Mar, 30202 Cartagena, Spain

Received 1 August 2001; received in revised form 19 June 2002

Abstract

This paper presents the experimental results carried out in dimpled tubes for laminar and transition flows and completes a previous work of the authors focused on the turbulent region. It was observed that laminar flow heat transfer through horizontal dimpled tubes is produced in mixed convection, where Nusselt number depends on both the natural convection and the entry region. Employing water and ethylene glycol as test fluids, the following flow range was covered: $x^* = 10^{-4}$–10^{-2} and $Ra = 10^6$–10^8.

The experimental results of isothermal pressure drop for laminar flow showed dimpled tube friction factors between 10% and 30% higher than the smooth tube ones. Moreover, it was perceived that roughness accelerates transition to critical Reynolds numbers down to 1400. Correlations for the laminar friction factor $f = f(Re, h/d)$ and for the critical Reynolds $Re_{crit} = Re_{crit}(h/d)$ are proposed. The hydraulic behaviour of dimpled tubes was found to depend mainly on dimple height.

In mixed convection, high temperature differences in the cross section were measured and therefore heat transfer was evaluated by a circumferentially averaged Nusselt number. Experimenal correlations for the local and the fully developed Nusselt numbers $\overline{Nu}_x = \overline{Nu}_x(x^*, Ra)$ and $\overline{Nu}_\infty = \overline{Nu}_\infty(Ra)$ are given. Results showed that at low Rayleigh numbers, heat transfer is similar to the smooth tube one whereas at high Rayleigh, enhancement produced by dimpled tubes can be up to 30%.

1. Introduction

Heat transfer enhancement through internally roughened tubes is an interesting technique in order to obtain more compact and efficient heat exchangers. Tubes with artificial roughness obtained by cold rolling the external tube surface are competitive in comparison to performance and cost of other enhanced techniques currently employed in turbulent flow.

There are two tube-side artificial roughness methods: two-dimensional roughness (transverse and helical ribs, helically corrugated and wire coil inserts) and three-dimensional roughness (sand-grain roughness, attached particle roughness, "cross-rifled" roughness and helically dimples).

Enhanced tubes can be used for many applications such as evaporators, condensers, oil radiators and heat exchangers for sterilising processes. This study is centred on improving heat exchangers used for sterilising organic fluids, through helically dimpled tubes. In these heat exchangers the organic fluid flows through tubes and is heated by steam or hot water flowing on the outside. Organic fluids usually show high viscosity and internal flow can be either laminar or turbulent at low Reynolds numbers. Therefore the tube-side film coefficient dominates the overall heat transfer coefficient.

Integral roughness techniques are suitable in turbulent flow but they are not effective in laminar flow because only the flow in the viscous boundary layer is mixed [1]. At any rate, pressure drop and heat transfer

* Corresponding author.
E-mail address: pedro.vicente@upct.es (P.G. Vicente).

0017-9310/02/$ - see front matter
PII: S0017-9310(02)00215-6

Nomenclature

A	heat transfer area, $(\pi d l_h)$ (m^2)
c_p	specific heat of the test fluid ($J\,kg^{-1}\,K^{-1}$)
d	envelope (maximum inside) diameter (m)
h	roughness height (Fig. 1) (m)
h_o	outside heat transfer coefficient ($W\,m^{-2}\,K^{-1}$)
h_i	inside heat transfer coefficient ($W\,m^{-2}\,K^{-1}$)
I	intensity (A)
k	thermal conductivity ($W\,m^{-1}\,K^{-1}$)
l	length between dimples (Fig. 1) (m)
l_p	length of test section between pressure taps (m)
l_h	length of the heat transfer section (m)
$\dot{m}$	mass flow rate of the test fluid ($kg\,s^{-1}$)
p	helical pitch (Fig. 1) (m)
ΔP	pressure drop across the test section ($N\,m^{-2}$)
Q	heat transfer rate (W)
q''	heat flux $(VI/\pi d l_h)$ ($W\,m^{-2}$)
t	temperature (K)
t_{wi}	inside surface temperature of the wall (K)
t_{wo}	outside surface temperature of the wall (K)
V	voltage (V)
U	overall heat transfer coefficient ($W\,m^{-2}\,K^{-1}$)
v	average velocity of the fluid ($m\,s^{-1}$)

Dimensionless groups

f	Fanning friction factor $(\Delta P d/2\rho v^2 l_p)$
Gr	Grashof number $(g\beta d^4 q''/v^2 k)$
Nu	Nusselt number $(h_i d/k)$
Pr	Prandtl number $(c_p \mu/k)$
Re	Reynolds number $(\rho v d/\mu)$
Ra	Rayleigh number $(Gr\ Pr)$
x^*	reduced length $(x/d\ Re\ Pr)$

Greek symbols

μ	dynamic viscosity ($kg\,m^{-1}\,s^{-1}$)
v	kinematic viscosity ($m^2\,s^{-1}$)
ρ	fluid density ($kg\,m^{-3}$)

Subscripts

a	augmented tube (dimpled tube)
b	based on bulk temperature
fc	forced convection
in	tube inlet
out	tube outlet
s	smooth tube
w	based on wall temperature
x	local value
∞	fully developed

design correlations for laminar flows are needed because:

- A roughened tube heat exchanger can be partially working in the laminar region. In viscous fluids, flow can be laminar in the entrance region where the fluid is cold and its viscosity is high.
- An existing enhanced heat exchanger could work at flow conditions outside from its design point.

Transition studies on dimpled tubes are needed to predict the critical Reynolds number. Artificial roughness techniques accelerate transition to critical Reynolds numbers down to 1500. When transition occurs, heat transfer increases suddenly and it can be up to 5 times higher than the smooth tube value corresponding to laminar flow.

Laminar flow heat transfer through horizontal tubes is usually influenced by buoyancy forces. The combined action of free and forced convection is called mixed convection and yields to heat transfer coefficients well above from those predicted by the constant density analysis. The dimensionless relation between buoyancy and viscous forces is given by Rayleigh number Ra. Mixed convection through horizontal tubes is characterised by the presence of two symmetrical recirculations in transversal direction to the mean flow. Secondary flow produces a heat transfer augmentation at the bottom and a reduction at the top of the tube; at uniform heat flux this implies that temperatures at the bottom are lower than at the top of the tube.

In laminar flow, the thermal entrance region, where the temperature profile changes axially, is usually important in comparison with the tube length. Here heat transfer is a function of the reduced distance to the entry given by x^*.

The experimental procedure to measure tube-side Nusselt numbers in mixed convection at laminar flows should be designed for taking into account both the inlet region and the free convection effects. Experimental points should be taken at different x^* of the thermally developing region to consider its influence on Nu. Moreover, to determine the buoyancy forces influence, tests should be carried-out in a wide range of Ra.

This paper presents the experimental results carried out in dimpled tubes for one-phase laminar and transitional flows and completes a previous work concerning turbulent flow, published by the authors at [2]. Employing water and ethylene glycol as test fluids, the following flow range was covered: $Re = 100$–$100,000$, $Pr = 2.5$–100, $x^* = 10^{-5}$–10^{-2} and $Ra = 10^6$–10^8.

Isothermal pressure drop experiments were carried out to study the roughness geometry influence on tube hydraulic behaviour: friction factors and critical Rey-

nolds numbers. The transition region was analysed in both pressure drop and heat transfer experiments. A thorough study centred in three dimpled tubes was enough to determine the dimpled tubes thermal behaviour for laminar flow.

2. Background

Three-dimensional roughness holds interest because of the high levels of enhancement and energy efficiency that can be obtained from its use, compared to the levels obtained by other passive enhancement geometric forms [1]. In fact, it turns out to be one of the best types of surface modifications for improving heat transfer performance in one phase turbulent forced convective flows.

Different types of three-dimensional roughness have been studied:

1. Roughness produced by knurling the inner tube surface: Cope [3].
2. Close-packed sand-grain-type roughness: Dipprey and Sabersky [4], Nikuradse [5].
3. Roughness by rolling copper tubes by internal mandrels: Takahashi et al. [6] and Cuangya et al. [7].
4. Roughness by rolling spaced protrusions on the outer surface (dimpled tubes): Kuwahara et al. [8], Rabas et al. [9], Olsson and Sundén [10].

Due to manufacturing costs, only helically dimpled tubes—for which dimples are formed by cold rolling deformation—are actually implemented in practical applications. Most of the above mentioned papers were focused on the turbulent region. Experiments were done in all cases using water or air as working fluids.

Only the paper of Olsson and Sundén [10] was centred on the laminar-transitional region $Re = 500$–6000. They studied small tubes for radiators, employing air as test fluid $Pr \approx 0.7$. Their measurements were highly influenced by the entry region. Since the flow behaviour presented a smooth transition, both friction factor and Nusselt number results were fitted to Re by a simple power series correlation. To extend the validity of heat transfer results, it was assumed that Nusselt number was proportional to $Pr^{1/3}$.

In the enhanced heat transfer literature, there are very few experimental works covering laminar and turbulent regimes simultaneously. Obot et al. [11] employed the results from 1950 to 1962 to study the role of transition in friction and heat transfer in rough tubes and noticed the lack of published data related to transition. They re-analysed the experimental data of Nunner [12] and Koch [13] on tubes with transverse ring inserts. They observed that the roughness height was the single most important parameter concerning on transition, with moderate effect of pitch.

The work of Manglik and Bergles [14,15] on twisted tapes, is an example of a complete study of an enhancement technique in laminar-transition-turbulent flows for a wide range of flow conditions (different Pr and Ra). The augmentation mechanism produced by insert devices is completely different to the one produced by integral roughness and therefore their results cannot be compared with those shown in this work.

Studies on laminar and turbulent regime in spirally fluted tubes have been carried out by several authors, results reported by Webb [1]. Obot et al. [16] studied the role of transition on spirally fluted tubes employing pressure drop and heat transfer results of other investigators. The transition point was clearly shown in the friction factor results by the presence of a local minimum. They assumed a Prandtl number influence on heat transfer of $Nu \propto Pr^{0.4}$.

To extend the use of an enhanced heat transfer technique to any tubular heat exchanger, its thermo-hydraulic behaviour should be known thoroughly and with the same reliability as the smooth tube is known. Heat exchanger designers should count on friction factor correlations $f = f(Re)$ in both laminar and turbulent regime, and should know the transition point. Heat transfer correlations should be available for laminar flows (usually in terms of $Nu = Nu(x^*, Ra)$) and for turbulent flows (usually in terms of $Nu = Nu(Re, Pr)$). Up to now the laminar-transition regime in integral roughened tubes has not been studied in detail. Normally only turbulent flow correlations (for $Re > 10,000$) are available for heat exchanger designers. Thus so they usually avoid designing in the laminar and transition region.

3. Experimental program

3.1. Tested tubes

The experimental study was carried out on a family of 10 enhanced tubes having dimples helically placed (dimpled tubes). Tubes were fabricated from stainless steel 316L plain tubes (inside diameter $d = 16$ mm, wall thickness $e = 1$ mm) and were plastically deformed by disks provided with protrusions, which were rolled on the outer tube surface.

Fig. 1 shows a sketch of a dimpled tube, where p stands for helical pitch; h, dimple height; and l, distance between dimples. Two non-dimensional parameters have been used to define tube roughness: reduced height h/d and dimple density d^2/pl. These parameters describing the tubes geometry are listed in Table 1.

The inside diameter d is the envelope diameter defined by Bergles et al. [17] which is the maximum inside diameter. This diameter has been used as the characteristic length to obtain the non-dimensional numbers Re, x^*, Ra, Nu and f.

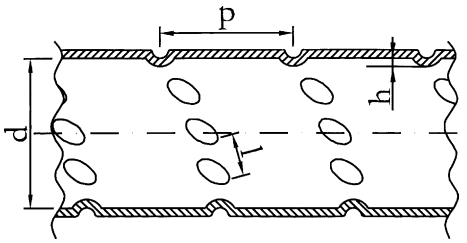

Fig. 1. Sketch of a dimpled tube.

Table 1
Geometry of tested tubes

Tube no.	d (mm)	h (mm)	p (mm)	l (mm)	h/d (–)	d^2/pl (–)
01	16.0	1.33	13.0	8.85	0.0831	2.225
02	16.0	1.58	13.1	8.99	0.0988	2.175
03	16.0	1.91	13.8	8.89	0.1194	2.085
04	16.0	1.28	14.6	8.91	0.0800	1.975
05	16.0	1.83	14.5	9.02	0.1144	1.964
06	16.0	1.59	17.2	9.02	0.0994	1.652
07	16.0	1.84	16.6	9.06	0.1150	1.700
08	16.0	1.87	16.8	8.90	0.1169	1.709
09	16.0	1.55	10.9	8.90	0.0969	2.646
10	16.0	1.64	11.4	8.76	0.1025	2.575

Besides, a smooth tube ($d = 16$ mm, $e = 1$ mm) was employed to check and to adjust the experimental set-up. Smooth tube results have been employed to determine the enhancement produced by dimpled tubes.

3.2. Experimental facility

A sketch of the experimental set-up is shown in Fig. 2. The facility consisted in two independent circuits: the main circuit where the test tubes were installed and the secondary circuit used for regulation.

The main circuit consisted of a variable-speed centrifugal pump, two oval wheels flowmeters and the test section. The working fluid was pumped from an open reservoir tank and then passed through one of the flowmeters into the test section. There, it was heated and returned to the tank.

Heat was added by Joule effect passing an alternating current directly through the tube wall. A 6 KVA transformer was connected to the tube by cooper electrodes. The length between electrodes defined the heat transfer tests section l_h and could be easily modified up to 4 m. An auto-transformer was connected to the transformer to regulate the power supply.

To keep a constant temperature in the tank, a cooling circuit was added. The secondary circuit consisted of a variable-speed centrifugal pump, a double-pipe heat exchanger and an electrical heater. The fluid was cooled by chilled water in the counterflow heat exchanger. The electrical heater, controlled by a PID, allowed the adjustment of the tank temperature to the desired value.

All temperatures were measured by resistive temperatures devices (RTD's). "A" class RTD's connected by four wires to an HP 34970A Data Acquisition Unit, ensured 0.08 °C accuracy. Fluid inlet and outlet temperatures t_{in}, t_{out} were measured by submerged type RTD's. Outside wall temperature was measured at one axial position by eight RTD's spaced 45°. These RTD's were fixed on the outer surface by a high thermal conductivity adhesive.

Overall electrical power added to the fluid, Q, was calculated by measuring voltage (0–15 V) and current (0–600 A). Fluid outlet temperature t_{out} can be indirectly calculated by an energy balance

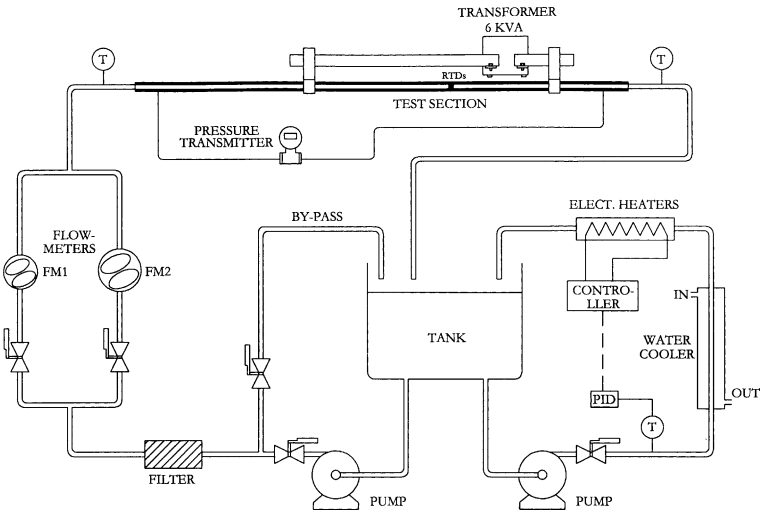

Fig. 2. A schematic diagram of the experimental set-up.

$$t_{out} = t_{in} + \frac{Q}{\dot{m}c_p}. \quad (1)$$

As the existing mixing chamber at the exit of the test section was not efficient enough in laminar flows, fluid outlet temperature t_{out} was in all cases determined by Eq. (1).

Pressure drop was measured along the pressure test section ($l_p = 5.2$ m) by means of a highly accurate pressure transmitter. Two differential pressure transmitters of different full scales, assured the accuracy of pressure drop measurements.

3.3. Experimental procedure

Uniform heat flux heat transfer and isothermal pressure drop tests were carried out by employing water and ethylene glycol as test fluids.

Pressure drop experiments were carried out to obtain isothermal friction factor data. In order to assure that measurements were taken at the fully developed region, upstream pressure tap was located 100 diameters away from a high curvature radius elbow. As *Re* depends largely on fluid viscosity, tests were carried out with water at 65 and 30 °C, and ethylene glycol at 55 and 30 °C, covering a continuous Reynolds range from 200 to 100,000. Isothermal fanning friction coefficients were determined from fluid flow rate and pressure drop measurements.

Heat transfer experiments in laminar flow were carried out to determine the local tube-side heat transfer coefficient under constant heat flux conditions.

A calibration test with no energy addition was done for each tube in order to calibrate the RTD's layout resistances as well as circuit heat loss. At high flow rates, wall temperature should be equal to fluid temperature ($t_w \approx t_b \approx t_{in} \approx t_{out}$). Therefore the differences between RTD's measurements and fluid temperature are due to the layout resistances. On the other side, at low flow rates differences up to 3 °C between fluid inlet and outlet temperatures were observed. A set of tests at low flow rates with different fluid temperatures allowed to calculate the heat transfer coefficient per unit length of the main circuit.

Due to accuracy reasons, experimental measurements were carried out with a minimum heat flux in order to have a fluid–wall difference of temperatures higher than 5 °C. This made buoyancy effects become important, and local Nusselt number was variable in the local section $Nu_x = Nu(x, \theta)$. A circumferential average Nusselt number $\overline{Nu}_x$ was defined as

$$\overline{Nu}_x = \frac{d}{k}\frac{q''}{\bar{t}_{wi}(x) - t_b(x)}, \quad (2)$$

where q'' is the circumferential average heat flux and $\bar{t}_{wi}$ is the mean inner-wall temperature.

The circumferential average outer-wall temperature $\bar{t}_{wo}$ was calculated as the mean value of the eight wall RTD's measurements placed on the same section. The number of RTD's and their size ($\approx 0.4d$), assured this procedure to be an accurate method to determine $\bar{t}_{wo}$. The circumferential average inner-wall temperature $\bar{t}_{wi}$ was numerically calculated by solving the steady-state one-dimensional heat conduction equation with heat generation in the tube wall.

Joule effect heating yields to a constant heat generation boundary condition. If the tube is properly insulated and the circumferential temperature gradients are not important, it can be assumed a uniform heat flux boundary condition. In mixed convection, high circumferential temperature gradients are presented (1 °C/mm), producing circumferential heat fluxes. Therefore the radial heat flux will not be uniform. Circumferential heat flux will increase the radial heat flux at the tube bottom; this intensifies the secondary flow which increases the heat transfer coefficient. Laminar flow film coefficients in horizontal tubes under UHF depend on the axial position in the thermally developing region and on buoyancy effects in the fully developed region. Nusselt number correlations are usually functions of reduced position x^* and Rayleigh number Ra ($Nu = Nu(x^*, Ra)$). In the experimental facility the local tube-side heat transfer coefficient was measured under uniform heat flux conditions. The objective of the tests was to obtain series of points to be correlated in the form ($Nu = Nu(x^*, Ra)$). Therefore, both the inlet region and the buoyancy effects have been considered.

Using water (WT) and ethylene glycol (EG), different series of data at different flow conditions were proposed, as shown in Table 2.

Around 200 experimental points ($\approx$40 per series) for each tube were carried out. This enables to obtain reliable correlations for both the thermally developing region ($Nu = Nu(x^*)$) and the fully developed region ($Nu = Nu(Ra)$). By combining both expressions, an equation in the form ($Nu = Nu(x^*, Ra)$) is obtained, valid for the flow range studied. The large Prandtl number range covered ($Pr = 6$–130) allowed the study of the Prandtl number influence on heat transfer.

Table 2
Series of experimental points

Series	Fluid	Ra	x^*	Pr
01	WT	8.0×10^6	10^{-3}–10^{-2}	6–7
02	WT	2.4×10^7	10^{-3}–10^{-2}	6–7
03	EG	4.0×10^6	10^{-4}–10^{-2}	90–130
04	EG	8.0×10^6	10^{-4}–10^{-2}	90–130
05	EG	1.6×10^7	10^{-4}–10^{-2}	90–130

3.4. Experimental uncertainty

Experimental uncertainty was calculated following Kline and McClintock [18] method based on a 95% confidence level. Instrumentation errors were as follows: temperature, 0.08 °C; flow rate, 0.4% full scale; differential pressure 0.075% span; intensity 0.1% measure + 0.04% full scale; and voltage, 0.04% measure + 0.03% full scale. An uncertainty of ±0.5% to ρ and ±1% to μ, c_p and k was assigned to the thermophysical properties of the tested fluids. An uncertainty of 0.1% was allocated to the inner diameter of the test tube. Test section length uncertainties were 5 mm for the pressure test section and 10 mm for the heat transfer test section.

An additional uncertainty was assigned to the calculation of the circumferential average outer-wall temperature $\bar{t}_{wo}$. It was assigned an uncertainty of 2.5% ($t_{w,up} - t_{w,do}$) where $t_{w,up}$ is the wall temperature in the upper point of the section and $t_{w,do}$ is the wall temperature in the lower point of the section.

Uncertainty calculations showed maximum values of 6% for Nusselt number, 3% for friction factor, 4% for Reynolds number, 3.5% for Prandtl number, 3.5% for reduced length x^* and 4.5% for Rayleigh number.

4. Pressure drop results

Isothermal pressure drop studies were performed for water and ethylene glycol within the range between $Re = 200$ to 100,000 in one smooth tube and 10 dimpled tubes. The measurements were taken at the hidrodynamically developed region and are presented in non-dimensional form as Fanning friction factor versus Reynolds number.

The experimental set-up was adjusted and verified through pressure drop experiments with a smooth tube. Laminar results were compared to the analytical solution ($f_s = 16/Re$) while results in the turbulent region were compared to Blasius equation ($f_s = 0.0791 Re^{-0.25}$). Smooth tube friction factor results are shown in Fig. 3 or 4. An excellent agreement with the mentioned correlations is observed: ±3% for 95% of the experimental data. The transition point is determined by the local minimum located at $Re_{s,crit} = 2100$. Friction factor results for the 10 dimpled tubes are plotted in Figs. 3 and 4. The results show that dimpled tubes accelerate the transition point. When critical Reynolds numbers for all the tubes were correlated, it was found that transition point depends on roughness geometry, mainly on dimple height (h/d), with a negligible influence of dimpled density (d^2/pl). The following correlation is proposed to predict critical Reynolds number in dimpled tubes:

$$Re_{a,crit} = 340.7(h/d)^{0.654}, \tag{3}$$

valid for the geometric range $(h/d) = 0.08$–0.12.

Eq. (3) is not suitable at low reduced height (h/d) values. As (h/d) decreases, the critical Reynolds number should approach to the asymptotic value corresponding to the smooth tube one. According to the procedure suggested by Churchill and Usagi [20], the following alternative correlation is proposed:

$$Re_{crit} = 2100[1 + 7.9 \times 10^7 (h/d)^{-6.54}]^{-0.1}. \tag{4}$$

Pressure drop for laminar flow produced by dimpled tubes is slightly higher than the one produced by smooth

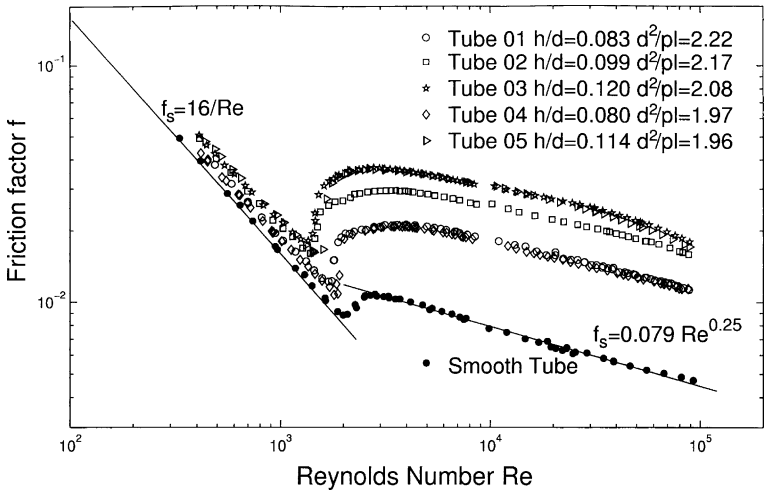

Fig. 3. Friction factor vs. Reynolds. Tubes 01–05.

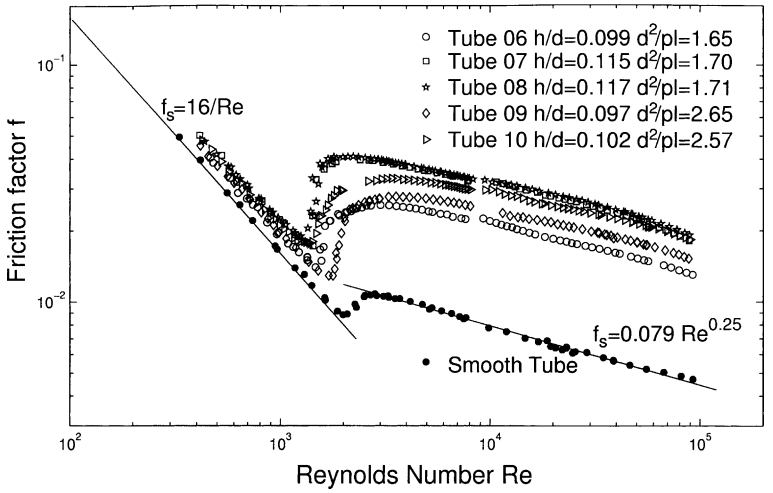

Fig. 4. Friction factor vs. Reynolds. Tubes 06–10.

tubes. Eq. (5) correlates the Fanning friction factor results for laminar flow of the ten dimpled tubes studied

$$f_a = f_s[1 + 123.2(h/d)^{2.2} Re^{0.2}]. \quad (5)$$

Friction factor augmentations between $f_a/f_s = 1.1$–1.3 for laminar flows were observed, depending on roughness geometry. However, turbulent flow pressure drop is much higher in dimpled tubes than in smooth tubes ($f_a/f_s = 2$–4). Turbulent friction factor results were analysed in detail by the authors in [2].

5. Heat transfer results

Heat transfer experiments were carried out for smooth and dimpled tubes for laminar flow at mixed convection following the experimental procedure described at Section 3.3. The objective of these tests was to obtain series of experimental points to achieve correlations in the form $Nu = Nu(x^*, Ra)$.

Fluid properties were evaluated at bulk temperature in the measure point, t_b. In order consider fluid viscosity variation in the heated section, experimental Nusselt number was corrected by the widely known correction factor $(\mu_w/\mu_b)^{0.14}$.

5.1. Smooth tube

Laminar heat transfer tests on a smooth tube have been carried out to check the facility capabilities as well as to verify the measurements uncertainties in mixed convection. Petukhov and Polyakov [19] included one chapter about laminar mixed convection and proposed the following equation for the circumferential averaged Nusselt number $\overline{Nu}_x$ for laminar mixed convection under uniform heat flux conditions:

$$\overline{Nu}_x = Nu_{x,fc}[1 + (Ra/B)^4]^{0.045}, \quad (6)$$

where $Nu_{x,fc}$ is the local Nusselt number in pure forced convection given by

$$Nu_{x,fc} = 4.36 + 1.31(x^*)^{-1/3} \exp(-13\sqrt{x^*}) \quad (7)$$

and B is a function of the reduced axial position x^*

$$B = 5.0 \times 10^3 (x^*)^{-1} \quad \text{if } x^* < 1.7 \times 10^{-3},$$
$$B = 1.8 \times 10^4 + 55(x^*)^{-1.7} \quad \text{if } x^* > 1.7 \times 10^{-3}.$$

In pure forced convection the fully developed region begins at $x^* \approx 0.1$; here Nusselt number reaches the widely known value of $Nu_x = 4.36$. However, in mixed convection the thermally developing region is much smaller (e.g. $x^* \approx 0.002$ for $Ra = 4 \times 10^6$). Nusselt number at the fully developed region $\overline{Nu}_\infty$, shows an asymptotic behaviour ($x^* \to \infty$, $B = 1.8 \times 10^4$), and Eq. (6) can be written as follows:

$$\overline{Nu}_\infty = 4.36[1 + (Ra/18,000)^4]^{0.045}. \quad (8)$$

From Eq. (7) it can be deduced that, in the entry region, the local Nusselt number is proportional to $(x^*)^{-1/3}$. On the other hand, Eq. (8) indicates that in the fully developed region $\overline{Nu}_x \propto Ra^{0.18}$.

Experimental results for laminar mixed convection through a horizontal smooth tube were compared to Petukhov and Polyakov [19] correlation (Eq. (6)). Figs. 5 and 6 show the series of experimental points carried out with water and ethylene glycol, respectively. Results in the entry region are not influenced by natural convection effects. Numerical solution for laminar flow in forced convection under uniform heat flux, shows a Nusselt dependency on the reduced axial length of $Nu \propto (x^*)^{-1/3}$. Therefore, Nusselt number in the entry

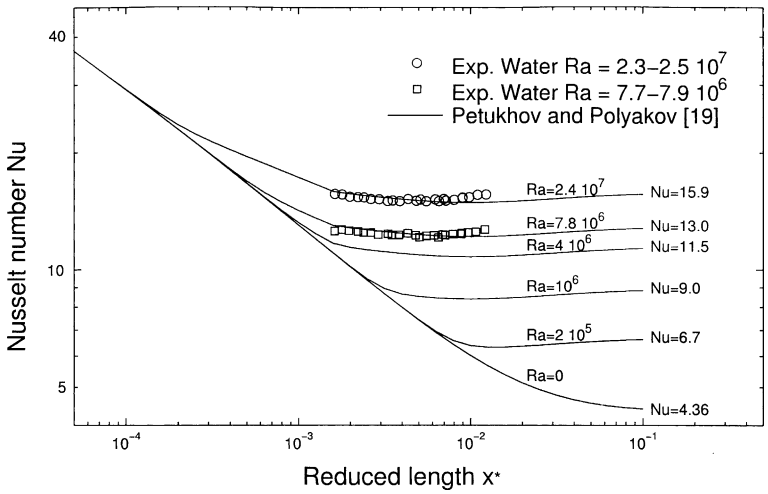

Fig. 5. $\overline{Nu}_x$ vs. x^*. Smooth tube water tests.

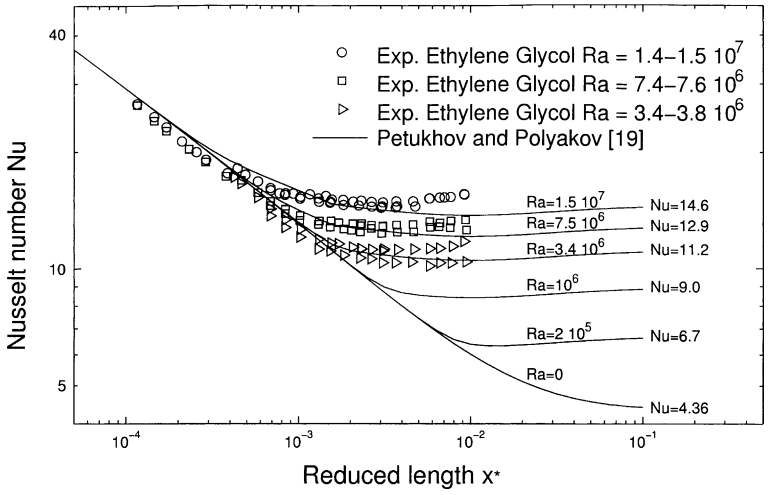

Fig. 6. $\overline{Nu}_x$ vs. x^*. Smooth tube ethylene glycol tests.

region was correlated in the form $Nu_x = C(x^*)^{-1/3}$ obtaining

$$\overline{Nu}_{x,\mathrm{fc}} = 1.27(x^*)^{-1/3}. \tag{9}$$

In the fully developed region, it was found that Nusselt numbers depended only on Rayleigh number. Results for water and ethylene glycol at $x^* > 0.002$ were correlated by

$$\overline{Nu}_\infty = 0.171Ra^{0.185}. \tag{10}$$

Eq. (10) can be combined with the pure forced convection asymptote ($Ra \to 0$, $Nu_\infty = 4.36$) by the method outlined by Churchill and Usagi [20] to yield

$$\overline{Nu}_\infty = 4.36[1 + (Ra/25,000)^{0.74}]^{0.25}. \tag{11}$$

Eq. (11), which represents the fully developed region ($x^* \to \infty$), can be combined with Eq. (9), which embodies thermal entrance effects ($x^* \to 0$), by the following correlation:

$$\overline{Nu}_x = (\overline{Nu}^{10}_{x,\mathrm{fc}} + \overline{Nu}^{10}_\infty)^{0.1}. \tag{12}$$

This equation correlates 95% of the experimental results of water and ethylene glycol within a deviation of ±6%.

In addition to the five series of the experimental points (Table 2), some experimental measurements in the fully developed region and different Rayleigh numbers were carried out. Fig. 7 shows these results as $\overline{Nu}_\infty$ at $x^* \approx 0.01$ for water and ethylene glycol in the range $Ra = 10^6$–10^8. Fully developed Nusselt number results are compared to Eq. (11) and to Petukhov and Polyakov [19].

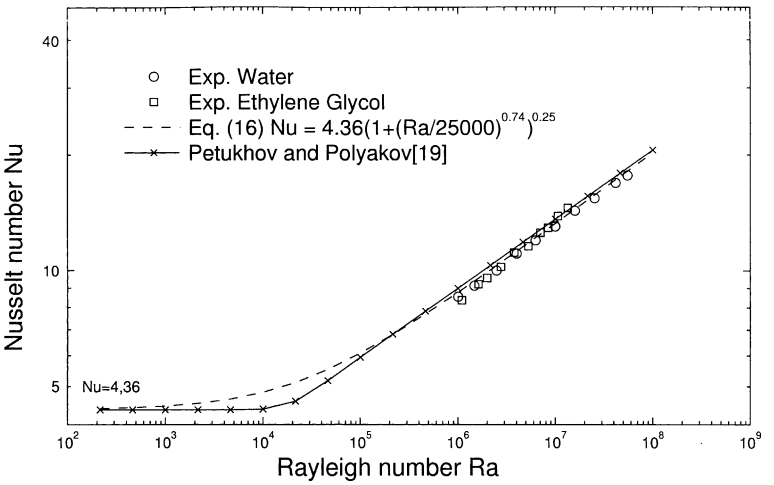

Fig. 7. $\overline{Nu}_\infty$ vs. *Ra*. Smooth tube.

These data extend the range of use of the correlations proposed to $Ra = 10^6$–10^8. Moreover, the asymptotic behaviour of $\overline{Nu}_x$ vs. x^* curve ($x^* \to 0$, $\overline{Nu}_x \propto (x^*)^{1/3}$ and $x^* \to \infty$, $\overline{Nu}_x = \overline{Nu}_\infty$) allows to consider that the proposed correlations are valid in the whole range of x^*.

5.2. Dimpled tubes

A heat transfer study in tubes 01, 02 and 03 has been carried out to determine the thermal behaviour of dimpled tubes in mixed convection. This experimental study in three tubes was enough to characterise the dimpled tube family for laminar and transition flow. The range of roughness geometry was: dimple height $h/d = 1.3$–1.9 and dimple density $d^2/pl \approx 2.1$ (Table 1).

In [2], it was shown that heat transfer in turbulent flow is highly increased up to augmentation factors of $Nu_a/Nu_s = 2.5$. In this work, pressure drop results showed that dimpled tubes accelerate transition down to 1400. Heat transfer results show transition acceleration to critical Reynolds numbers similar to pressure drop results.

Dimpled tube results showed that natural convection effects were of great importance in the flow behaviour. Downstream the entry region, wall temperature measurements were much higher close to the upper generatrix than in the region near to the lower generatrix. Circumferential temperature variations up to 20 °C were measured. The measuring section consisted on 8 RTD's spaced 45° and $0.4d$ wide. The outer tube wall was completely surrounded by the set of RTD's. This assured a properly averaged wall temperature. In the same way, the RTD's size averaged the punctual temperature variations induced by the dimples.

Dimpled tubes behaviour in laminar heat transfer is similar to the smooth tube one. Thus, heat transfer is evaluated by the circumferential average Nusselt number that depends on entry region (x^*) and buoyancy forces (*Ra*).

Figs. 8 and 9 show, as an example of the measurements, heat transfer experimental results from Tube 02. Results are presented in terms of Nu_a vs. x^* for the different Rayleigh numbers, using water and ethylene glycol as working fluids. Experiments were carried out following the same procedure as for the smooth tube tests. The flow range studied was $x^* = 10^{-4}$–10^{-2} and $Ra = 4$–24×10^6. A Prandtl number range of $Pr = 6$–130, made possible to determine its influence on heat transfer.

Heat transfer in the *thermally developing region* was not influenced by natural convection. Experimental measurements that presented temperature wall differences lower than 1 °C were supposed to belong to the entry region. It is observed that when they are plotted as Nu_a vs. x^*, the tendency follows the smooth tube trend. An expression of the type $Nu_x = C(x^*)^{-1/3}$ was used to correlate the pure forced convection points. The following correlation which is valid for all three dimpled tubes was proposed:

$$\overline{Nu}_{x,\mathrm{fc}} = 1.22(x^*)^{-1/3}. \tag{13}$$

The Nusselt number in pure forced convection for the dimpled tubes is around 4% lower than in the smooth tube. Dimples increase pressure drop and consequently the energy added to the fluid. This results in an acceleration of the thermal profile development. Thus, the thermally developing region is shorter and the Nusselt number decreases faster. Water and ethylene glycol results in the *fully developed region* ($x^* > 0.002$) were correlated using a particular statistical regression for each tube. By applying Churchill and Usagi [20] method, these correlations are combined to the smooth tube

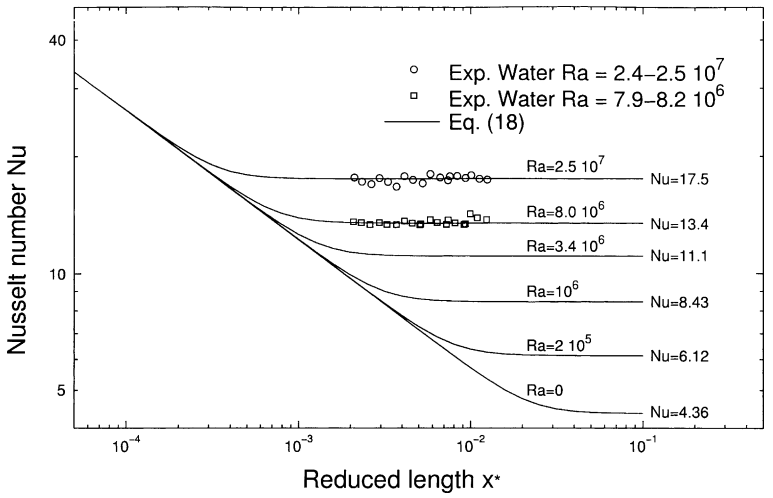

Fig. 8. $\overline{Nu}_x$ vs. x^*. Tube 02 water tests.

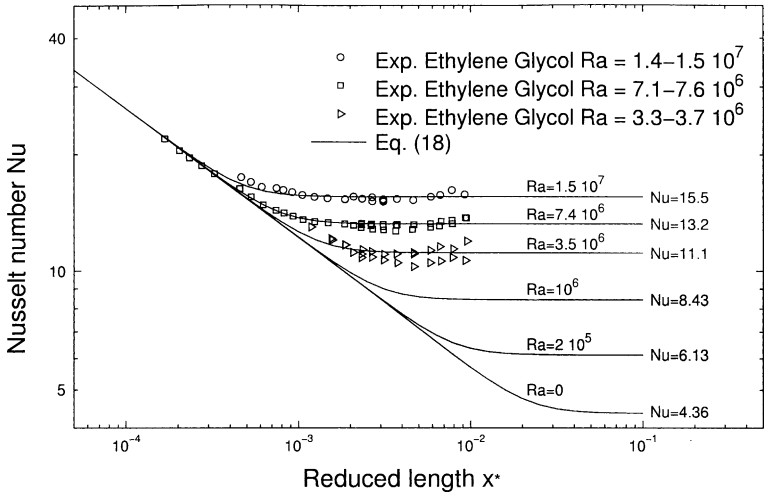

Fig. 9. $\overline{Nu}_x$ vs. x^*. Tube 02 ethylene glycol tests.

solution in pure forced convection ($\overline{Nu}_\infty = 4.36$ for $Ra \to 0$) to give

$$\text{Tube 01} \quad \overline{Nu}_\infty = 4.36[1 + (Ra/62,500)^{0.936}]^{0.25}, \tag{14}$$

$$\text{Tube 02} \quad \overline{Nu}_\infty = 4.36[1 + (Ra/63,500)^{0.930}]^{0.25}, \tag{15}$$

$$\text{Tube 03} \quad \overline{Nu}_\infty = 4.36[1 + (Ra/56,500)^{0.947}]^{0.25}. \tag{16}$$

Results show a negligible influence of tube roughness on heat transfer for laminar mixed convection flow. In fact, differences among results of different geometries are in the range of experimental facility uncertainty. The following equation is proposed to correlate the Nusselt number at the fully developed region:

$$\overline{Nu}_\infty = 4.36[1 + Ra/67,000]^{0.24}. \tag{17}$$

This equation correlates 95% of the experimental results within a 6% deviation. When the thermally developing region is relatively small in comparison to the heat exchanger length, the fully developed Nusselt number $\overline{Nu}_\infty$ is assumed to be the mean Nusselt number and be calculated by Eq. (17).

It is convenient to develop a unique equation valid for the whole range of x^* and Ra that can be easily implemented in a computer program. By using once more the Churchill and Usagi [20] method, both correlations of the fully developed region (Eqs. (14)–(16)), and the thermally developing region (Eq. (13)) can be combined by the following correlation:

$$\overline{Nu}_x = \left(\overline{Nu}_{x,\mathrm{fc}}^{10} + \overline{Nu}_\infty^{10}\right)^{0.1}, \tag{18}$$

valid for the experimental studied range.

Following the same procedure than the one used in the smooth tube, some additional experimental measurements in the fully developed region ($x^* \approx 0.01$) and different Rayleigh numbers ($Ra = 10^6$–10^8) were carried out for all tubes. Fig. 10 shows, as an example of the measurements, $\overline{Nu}_\infty$ results for Tube 02. These results are compared to the correlation previously developed (Eq. (16)) and to Petukhov and Polyakov [19] equation.

These data extend the range of Eqs. (14)–(18) to $Ra = 10^6$–10^8. Moreover, the asymptotic behaviour of $\overline{Nu}_x$ vs. x^* allows the use of the equations for any value of x^* with a reasonable level of accuracy.

Fig. 11 plots $\overline{Nu}_\infty$ correlations developed for the smooth and the three dimpled tubes. It is observed that the slope of the curves is relatively different in dimpled tubes ($\overline{Nu} \propto Ra^{0.235}$) that in the smooth tube ($\overline{Nu} \propto Ra^{0.185}$).

Heat transfer augmentation produced by dimpled tubes in the fully developed region is shown in Fig. 12. Heat transfer in mixed convection through horizontal tubes is much higher than in pure force convection. The gravity body force produces two recirculations in transversal direction to the main flow. This secondary flow is mainly induced by the buoyancy forces resulting from the high temperature gradients near the wall. At low Rayleigh numbers, the secondary flow is weak and it can be diminished or decelerated by dimples. This will reduce the heat transfer coefficient. At high Rayleigh numbers, the secondary flow is well established and dimples increase the heat transfer.

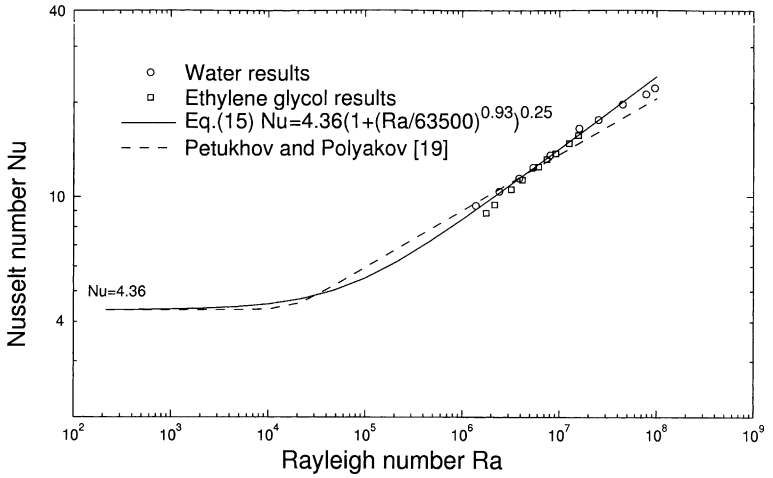

Fig. 10. $\overline{Nu}_\infty$ vs. Ra. Tube 02 results.

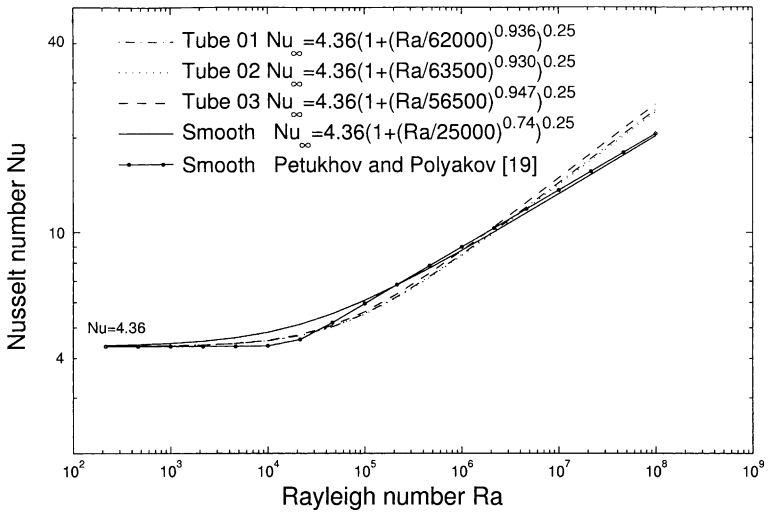

Fig. 11. Correlations proposed for $\overline{Nu}_\infty$.

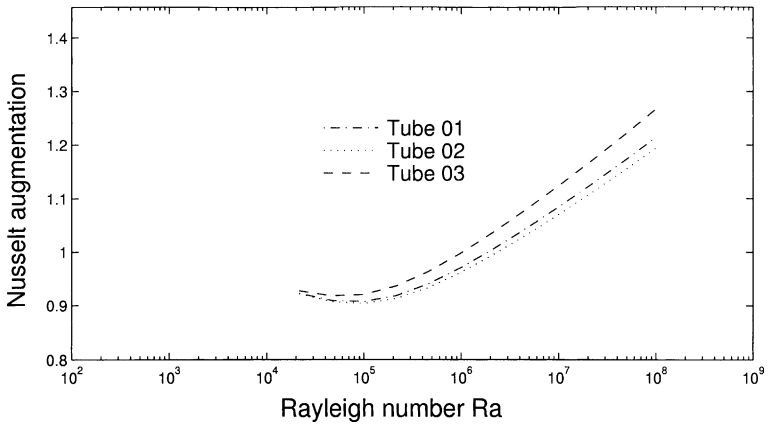

Fig. 12. Heat transfer augmentation vs. *Ra*. Dimpled tubes.

6. Overall heat transfer results

This paper presents the experimental results carried out in dimpled tubes for laminar and transition flows and completes the previous work of the authors [2] centred on the turbulent region. Heat transfer results for laminar, transition and turbulent flows, have been presented together in terms of *Nu* vs. *Re*; Figs. 13–16 show results for the smooth tube and dimpled tubes 01, 02 and 03. Flow conditions covered were: in laminar flow $Re = 100$–Re_{crit}, $Ra = 3.4$–15×10^6 and in turbulent flow $Re = Re_{crit}$–$100,000$, $Pr = 2.9$–92.

Nusselt number results in laminar mixed convection should be correlated in the form $\overline{Nu}_x = \overline{Nu}_x(x^*, Ra)$. However, in order to study transition at heating conditions, laminar Nusselt number results are presented in the form $\overline{Nu}_x = \overline{Nu}_x(Re, Ra)$. These results correspond to the measurements at a section located at $x/d = 100$ where the flow is fully developed.

Turbulent flow results for the whole dimpled tubes family were correlated in [2] by using an equation in the form $Nu = Nu(Re, Pr)$.

At low Reynolds, laminar flow Nusselt number in dimpled tubes shows a constant value depending on *Ra*.

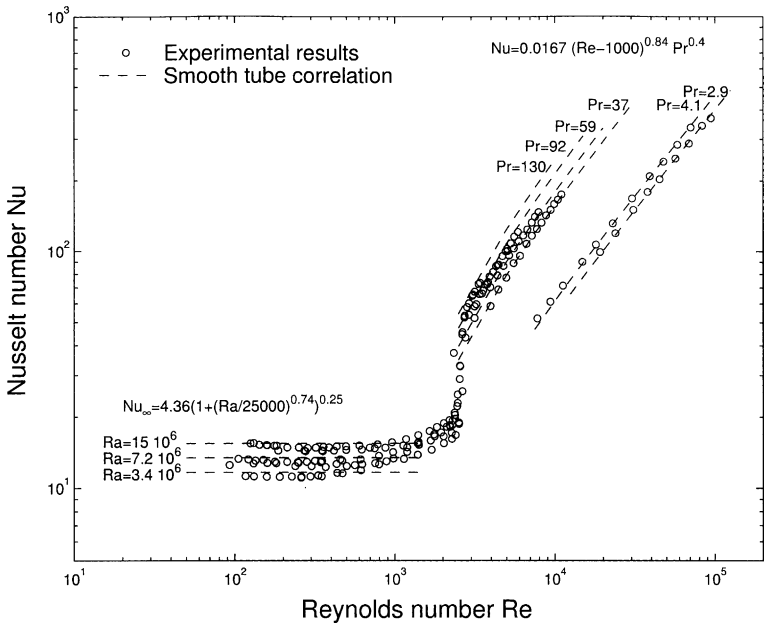

Fig. 13. Complete heat transfer results. Smooth tube.

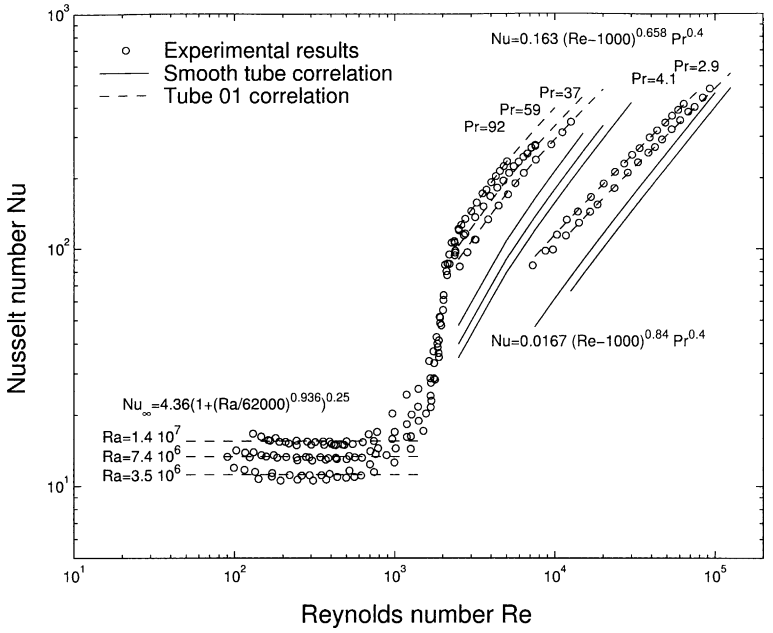

Fig. 14. Complete heat transfer results. Tube 01.

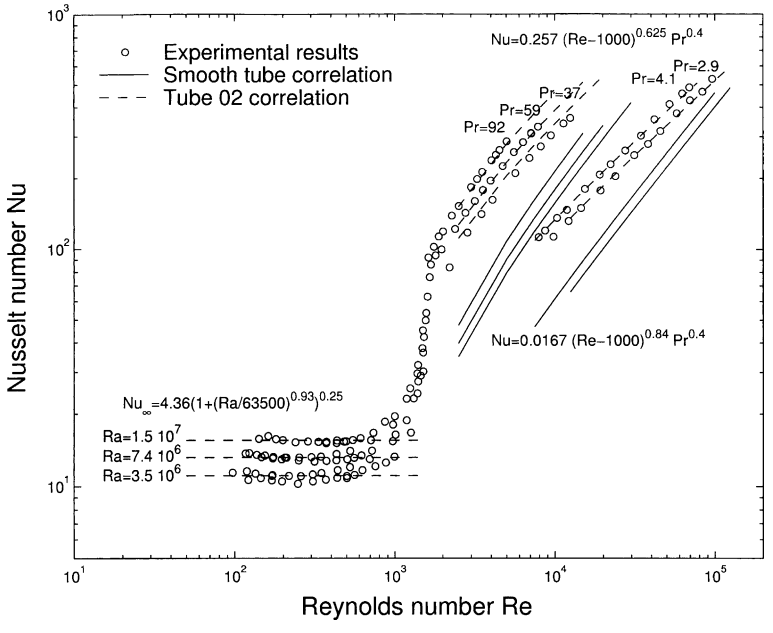

Fig. 15. Complete heat transfer results. Tube 02.

Fully developed Nusselt numbers for each dimpled tube were correlated by Eqs. (14)–(16). At Reynolds numbers from $Re \approx 700$ to Re_{crit}, Nusselt number rises. It was established that this change in the asymptotic behaviour was produced by the viscosity reduction in the boundary layer when heat was applied and not by entrance region effects $(Re \propto (x^*)^{-1})$.

Figs. 14–16 show that transition point does not depend apparently on Rayleigh (heat flux) and it appears at the same critical Reynolds number as it was observed at the isothermal pressure drop measurements. When flow becomes turbulent, heat transfer increases suddenly and it is up to 5 times higher than the smooth tube value corresponding to laminar flow. At the turbulent region,

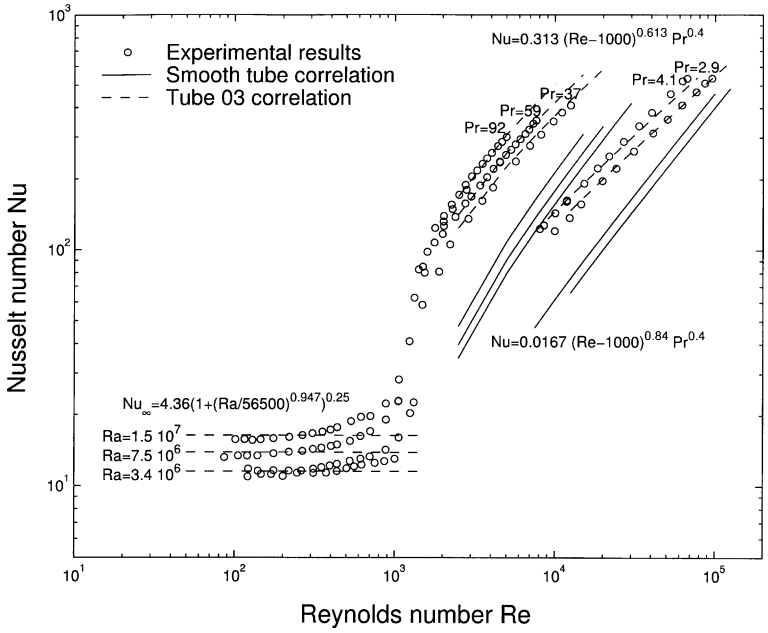

Fig. 16. Complete heat transfer results. Tube 03.

dimpled tubes present heat transfer augmentations up to 250% at low Reynolds numbers.

7. Conclusions

1. Pressure drop experimental results in ten dimpled tubes for laminar flow were reduced and a correlation in the form $f_a = f_a(Re, h/d)$, valid for $Re < Re_{crit}$ and $h/d < 0.12$ was proposed. Friction factor augmentations up to 30% were observed depending mainly on dimple height.
2. It was observed that dimpled tubes accelerate transition to critical Reynolds numbers down to 1400. A correlation for determining the critical Reynolds number was proposed in the form $Re_{crit} = Re_{crit}(h/d)$ valid for $h/d < 0.12$.
3. An experimental heat transfer investigation on three dimpled tubes was enough to study the dimpled tubes performance in the laminar region. Dimpled tubes present a similar behaviour than the smooth tube; heat transfer is produced in mixed convection where both entrance region and buoyancy effects are important. Results for each tube were reduced and correlated by equations of the type $\overline{Nu}_x = \overline{Nu}_x(x^*, Ra)$. Heat transfer augmentation depends on Rayleigh number; at high Rayleigh numbers, Nu augmentations up to 30% were obtained whereas at low Rayleigh numbers, Nusselt number was even lower.
4. Measurements were carried out at different Prandtl numbers ($Pr = 6$–130) and it was obtained that Nusselt number dependence on Pr and Gr is the same. Therefore it is possible to correlate Nusselt number as a function of an unique non-dimensional parameter $(Nu = f(Ra))$.
5. The present study on a dimpled tube family for Laminar and transition flows comes to complete the authors' previous work [2] focused on the turbulent region. The family of dimpled tubes with similar geometry to those which have been studied in the current work has been completely characterised. The proposed correlations for pressure drop and heat transfer can be directly used for design purposes, with a high level of accuracy and under a wide range of flow conditions: $Re = 100$–$100,000$, $Pr = 2.5$–100, $x^* = 10^{-5}$–10^{-2} and $Ra = 10^6$–10^8.

Acknowledgements

This research has been partially financed by the 1FD1997-0211 (TYP) grant of the "Dirección General de Enseñanza Superior e Investigatión Científica" in Spain and the HRS Spiratube company from Murcia (Spain).

References

[1] R.L. Webb, in: Principles of Enhanced Heat Transfer, first ed., Wiley Interscience, New York, 1994, p. 556.
[2] P.G. Vicente, A. Garcia, A. Viedma, Heat transfer and pressure drop for low Reynolds turbulent flow in helically

dimpled tubes, Int. J. Heat Mass Transfer 45 (2002) 543–553.
[3] W.G. Cope, The friction and heat transmision coefficients of rough pipes, Proceedings of the Institute of Mechanical Engineers 145 (1945) 99–105.
[4] D.F. Dipprey, R.H. Sabersky, Heat and momentum transfer in smooth and rough tubes at various Prandtl numbers, International Journal of Heat and Mass Transfer 6 (1963) 329–353.
[5] J. Nikuradse, Laws of flow in rough pipes, VDI Forschungsheft 361 (1933). English translation, NACA TM-1292 (1965).
[6] K. Takahashi, W. Nakayama, H. Kuwahara, Enhancement of forced convective heat transfer in tubes having three-dimensional spiral ribs, Heat Transfer Japanese Research 17 (1988) 12–28.
[7] L. Cuangya, G. Chuanyun, W. Chaosu, H. Jinshu, J. Cun, Experimental investigation of transitional flow heat transfer of three-dimensional internally finned tubes, in: Advances in Heat Transfer Augmentation and Mixed Convection, ASME Symposium, HTD-vol. 169, 1991, pp. 45–48.
[8] H. Kuwakara, K. Takahashi, T. Yanagida, T. Nakayama, S. Hzgimoto, K. Oizumi, Method of producing a heat transfer tube for single phase-flow, US Patent 4,794,775, 3 January 1989.
[9] T.J. Rabas, R.L. Webb, P. Thors, N.K. Kim, Influence of roughness shape and spacing on the performance of three-dimensional helically dimpled tubes, J. Enhanc. Heat Transfer 1 (1993) 53–64.
[10] C.O. Olsson, B. Sundén, Heat transfer and pressure drop characteristics often radiator tubes, Int. J. Heat Mass Transfer 39 (1996) 3211–3220.
[11] N.T. Obot, E.B. Esen, T.J. Rabas, The role of transition in determining friction and heat transfer in smooth and rough passages, Int. J. Heat Mass Transfer 33 (1990) 2133–2143.
[12] W. Nunner, Heat transfer and pressure drop in rough tubes, AERE Lib/Trans. (1990) 786.
[13] R. Koch, Pressure loss and heat transfer for turbulent flow, AEC-tr-3875 (1960).
[14] R.M. Manglik, A.E. Bergles, Heat transfer and pressure drop correlations for twisted-tape inserts in isothermal tubes: Part I—laminar flows, ASME J. Heat Transfer 115 (1993) 881–888.
[15] R.M. Manglik, A.E. Bergles, Heat transfer and pressure drop correlations for twisted-tape inserts in isothermal tubes: Part II—transition and turbulent flows, ASME J. Heat Transfer 115 (1993) 881–888.
[16] N.T. Obot, E.B. Esen, K.H. Snell, T.J. Rabas, Pressure drop and heat transfer for spirally fluted tubes including validation of the role of transition, Fouling and enhancement interactions, in: T.J. Rabas, J.M. Chenoweth (Eds.), ASME Symposium, HTD-vol. 164, ASME, New York, 1991, pp. 85–92.
[17] A.E. Bergles, A.R. Blumenkrantz, J. Taborek, Performance evaluation criteria for enhanced heat transfer surfaces, Heat Transfer 2 (1974) 239–243.
[18] S.J. Kline, F.A. McClintock, Describing uncertainties in single sample experiments, Mech. Eng. 75 (1953) 3–8.
[19] B.S. Petukhov, A.F. Polyakov, in: Heat Transfer in Turbulent Mixed Convection, Hemisphere, New York, 1988, p. 216.
[20] S.W. Churchill, R. Usagi, A general expression for the correlation of rates of transfer and other phenomena, AIChE J. 18 (1972) 1121–1128.